and the lack of correlation in Figure 5a is likely due to the lower stabilization energy (compared with the other complexes) for the LUMO-based MLCT state. For DP and taphen complexes, however, it seems more likely that the lack of correlation also implies a different nature of the orbitals involved in the electrochemical reduction and light absorption processes.

Concerning the correlation between emission energy and reduction potential (Figure 5b) it can be noted that the complexes of i-biq and DP behave again in an anomalous way, while the taphen complex apparently follows the linear relationship obeyed by the other complexes. The luminescence lifetime of the Ru(i-biq)$_3^{2+}$ shows that the emitting excited state is largely ligand centered in character.[34] This inversion in the energy ordering between MLCT and LC levels in passing from the singlet to the triplet manifold is not unexpected because of the larger singlet–triplet splitting of the LC states. The smaller distance from the straight line of the i-biq point (compare parts a and b of Figure 5) is in agreement with the coming into play of a lower energy LC excited state.

For the DP complex, the emission is apparently CT in nature. Comparison between parts a and b of Figure 5 suggests that the same orbital (or energetically similar orbitals) is involved in the absorption and emission process. As we have seen above, the most likely explanation for the absorption properties assumes the involvement of the free ligand SLUMO, whereas excited-state absorption spectra have shown that the excited electron is largely localized on the phenazine moiety of the ligand,[35] i.e. on the LUMO orbital. The lack of correlation between emission and redox energies seems to imply that the observed luminescence does not come from the CT excited state involving the LUMO, but from a higher energy (thermally activated) excited state. A possible explanation would involve a smaller excited-state distortion for this complex (and hence Stokes shift) due to the very extended fused-ring structure of the ligand.[36]

Figure 5b shows that the taphen complex apparently is well-behaved in the correlation between emission energy and redox potential. This is quite surprising because even if the same (LUMO) orbital is involved in the emission and reduction processes, one expects a lack of correlation as in Figures 6a and 7 because of the small Q value (Table I). We believe that a plausible explanation may be the following. The LUMO of taphen is strongly localized on the N=N bridge (Figure 2) of the molecule (the p_N values in the 5- and 6-positions are +0.56 and −0.56),[37] which implies that the reduced ligand is strongly distorted along the N_5–N_6 bond. As a consequence, in the taphen complex the minimum of the potential energy surface of the ^{3}MLCT excited state involving the LUMO should be strongly displaced compared to that of the ground state, thus decreasing the energy of the emission maximum. This apparently compensates for the expected higher emission energy due to the smaller Q value. This explanation is consistent with the results obtained for the temperature dependence of the luminescence of taphen–Ru(II) complexes discussed in a previous paper.[37]

Acknowledgment. We wish to thank G. Gubellini for the drawings. This work was supported by the Consiglio Nazionale delle Ricerche and Ministero della Pubblica Istruzione (Italy) and the Swiss National Science Foundation.

Registry No. i-biq, 35202-46-1; bpy, 366-18-7; phen, 66-71-7; 4,4′-dpb, 6153-92-0; bpym, 34671-83-5; pq, 7491-86-3; biq, 119-91-5; bpz, 10199-00-5; DP, 19535-47-8; taphen, 653-05-4; Ru(i-biq)$_3^{2+}$, 82762-29-6; Ru(i-biq)$_2$(bpy)$^{2+}$, 89340-69-2; Ru(phen)$_3^{2+}$, 22873-66-1; Ru(bpy)$_2$(4,4′-dpb)$^{2+}$, 93461-97-3; Ru(bpy)$_2$(bpym)$^{2+}$, 65013-22-1; Ru(bpy)$_2$(pq)$^{2+}$, 74171-82-7; Ru(bpy)$_2$(biq)$^{2+}$, 75777-90-1; Ru(bpy)$_2$(bpz)$^{2+}$, 85335-53-1; Ru(bpy)$_2$(DP)$^{2+}$, 87564-74-7; Ru(bpy)$_2$(taphen)$^{2+}$, 98914-20-6.

(34) Belser, P.; von Zelewsky, A.; Juris, A.; Barigelletti, F.; Tucci, A.; Balzani, V. *Chem. Phys. Lett.* **1982**, *89*, 101.
(35) Chambron, J.-C.; Sauvage, J.-P.; Amouyal, E.; Koffi, P. *Nouv. J. Chim.* **1985**, *9*, 527.
(36) We thank one of the reviewers for suggesting this point.
(37) Barigelletti, F.; Juris, A.; Balzani, V.; Belser, P.; von Zelewsky, A. *J. Phys. Chem.* **1986**, *90*, 5190.

Notes

Contribution from the Department of Chemistry, Thimann Laboratories, University of California, Santa Cruz, California 95064, and Department of Chemistry and Biochemistry, University of Windsor, Windsor, Ontario, Canada N9B 3P4

Synthesis, Structure, and Properties of Tetraphenylphosphonium Tetrakis(2-mercaptopropionato)trinickelate(II), $(Ph_4P)_2[Ni_3(SCH(CH_3)COO)_4]$: A Linear Trimeric Thiolato Complex of Nickel

Steven G. Rosenfield,[†] Maria L. Y. Wong,[‡] Douglas W. Stephan,[‡] and Pradip K. Mascharak*[†]

Received June 5, 1987

Our interest in synthesis of discrete thiolato complexes of divalent nickel stems from the occurrence of a S-ligated nickel center at the active site of the Ni-containing hydrogenases.[1-7] In a previous paper,[8a] we have reported the convenient synthesis and properties of distorted tetrahedral arenethiolates of the type $[Ni(SAr)_4]^{2-}$. Recently, we have also reported the syntheses, structures, and spectral characteristics of two distorted octahedral Ni(II) thiolato complexes.[9] Though attempts to model the active site of the enzyme(s) are directed toward synthesis of mononuclear nickel complexes, interest in the chemistry of nickel thiolates has resulted in multinuclear nickel–thiolato species with novel

[†] University of California.
[‡] University of Windsor.

(1) Thomson, A. J. *Nature (London)* **1982**, *298*, 602.
(2) (a) Graf, E.; Thauer, R. K. *FEBS Lett.* **1981**, *136*, 165. (b) Albracht, S. P. J.; Graf, E.-G.; Thauer, R. K. *FEBS Lett.* **1982**, *140*, 311. (c) Kojima, N.; Fox, J. A.; Hausinger, R. P.; Daniels, L.; Orme-Johnson, W. H.; Walsh, C. *Proc. Natl. Acad. Sci. U.S.A.* **1983**, *80*, 378.
(3) Lancaster, J. R., Jr. *Science (Washington, D.C.)* **1982**, *216*, 1324.
(4) Kruger, H.-J.; Huynh, B. H.; Ljungdahl, P. O.; Xavier, A. V.; Der Vartanian, D. V.; Moura, I.; Peck, H. D., Jr.; Teixeira, M.; Moura, J. J. G.; LeGall, J. *J. Biol. Chem.* **1982**, *257*, 14620.
(5) Unden, G.; Bocher, R.; Knecht, J.; Kroger, A. *FEBS Lett.* **1982**, *145*, 230.
(6) (a) Cammack, R.; Patil, D.; Aguirre, R.; Hatchikian, E. C. *FEBS Lett.* **1982**, *142*, 289. (b) LeGall, J.; Ljungdahl, P. O.; Moura, I.; Peck, H. D.; Jr.; Xavier, A. V.; Moura, J. J. G.; Teixeira, M.; Huynh, B. H.; Der Vartanian, D. V. *Biochem. Biophys. Res. Commun.* **1982**, *106*, 610. (c) Moura, J. J. G.; Moura, I.; Huynh, B. H.; Kruger, H.-J.; Teixeira, M.; Du Varney, R. C.; Der Vartanian, D. V.; Xavier, A. V.; Peck, H. D., Jr.; LeGall, J. *Biochem. Biophys. Res. Commun.* **1982**, *108*, 1388. (d) Teixeira, M.; Moura, I.; Xavier, A. V.; Der Vartanian, D. V.; LeGall, J.; Peck, H. D., Jr.; Huynh, B. H.; Moura, J. J. G. *Eur. J. Biochem.* **1983**, *130*, 481.
(7) Albracht, S. P. J.; Albracht-Ellmer, K. J.; Schmeeding, D. J. M.; Slater, E. C. *Biochim. Biophys. Acta* **1982**, *681*, 330.
(8) (a) Rosenfield, S. G.; Armstrong, W. H.; Mascharak, P. K. *Inorg. Chem.* **1986**, *25*, 3014. (b) Yamamaura, T.; Miyamae, H.; Katayama, Y.; Sasaki, Y. *Chem. Lett.* **1985**, *269*.
(9) Rosenfield, S. G.; Berends, H. P.; Gelmini, L.; Stephan, D. W.; Mascharak, P. K. *Inorg. Chem.* **1987**, *26*, 2792.

0020-1669/87/1326-4119$01.50/0

structures and properties.[10] Discrete polynuclear thiolato complexes containing two,[11] three,[11b,12-15] four,[16] six,[17] and eight[18] nickel atoms have been reported. In an attempt to synthesize the nickel complex of 2-mercaptopropionic acid (commonly known as thiolactic acid (**1**)), we have isolated a linear trimeric complex of

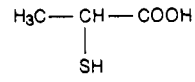

1

the composition $(Ph_4P)_2[Ni_3(SCH(CH_3)COO)_4]$ (**2**) in which the ligand is the doubly deprotonated anion of **1**. In this paper we report the synthesis, structure, and spectral properties of this trimeric complex. Linear trimeric thiolato complexes of nickel reported so far include $[Ni_3(SCH_2CH_2NH_2)_4]^{2+}$ (**3**),[14] $[Ni_3(SCH_2CH_2CH_2NH_2)_4]^{2+}$ (**4**),[15] $[Ni_3(S_2\text{-}o\text{-}xyl)_4]^{2-}$ (**5**),[12b] $[Ni_3(SCH_2CH_3)_8]^{2-}$ (**6**),[11b] and $[Ni_3(SCH_2CH_2S)_4]^{2-}$ (**7**).[12c]

Experimental Section

Preparation of Compounds. (±)-Thiolactic acid (**1**) was procured from Aldrich Chemical Co. and was used without further purification. $(Ph_4P)_2NiCl_4$ was synthesized by following a standard procedure.[19] In the following preparations, freshly distilled and degassed solvents were used. All manipulations were performed under an atmosphere of dry and pure dinitrogen.

$(Ph_4P)_2[Ni_3(SCH(CH_3)COO)_4]$ (2). A 190-μL (227-mg, 2.14-mmol) amount of thiolactic acid was added to a solution of 4 mmol of sodium methoxide (92 mg of sodium, 4 mmol) in 30 mL of methanol. After the mixture was stirred for 10 min, a 1.5-g (4-mmol) sample of Ph_4PCl was added to it. The solvent was removed in vacuo following 30 min of stirring. Addition of 30 mL of warm (~40 °C) acetonitrile to the sticky off-white residue and vigorous stirring (1 h) resulted in a pale yellow solution of the thiolate with NaCl suspended in it. Next, a solution of 880 mg (1 mmol) of $(Ph_4P)_2NiCl_4$ in 30 mL of acetonitrile was *slowly* added to the thiolate solution with continuous stirring. The initial pale yellow color gradually changed into deep greenish brown as the addition continued. After the entire amount of nickel was added, NaCl was removed by filtration and the volume of the deep greenish brown filtrate was reduced to ~30 mL. Finally, an additional batch of 290 mg (0.33 mmol) of $(Ph_4P)_2NiCl_4$ in 15 mL of acetonitrile was slowly added to the greenish brown solution to achieve a nickel-to-ligand ratio of 1:1.5. Precipitation of dark microcrystalline solid started almost immediately. The greenish black mixture was cooled at −20 °C for 4 h, and the dark solid was collected by filtration. A 500-mg (91%) yield of crude product was obtained. Slow diffusion of diethyl ether into DMF solution afforded 275 mg (60%) of large black blocks, mp 230–235 °C dec. Anal. Calcd for $C_{60}H_{56}O_8S_4P_2Ni_3$: C, 56.66; H, 4.44; Ni, 13.86. Found: C, 56.64; H, 4.44; Ni, 13.70. Selected IR bands (KBr pellet, cm^{-1}): 1640 (ν_{CO}, vs), 1490 (m), 1440 (m), 1300 (w), 1120 (m), 1000 (w), 880 (w), 760 (m), 720 (vs), 690 (s), 530 (vs), 420 (w).

Physical Measurements. Absorption spectra were recorded on a Perkin-Elmer Lambda 9 spectrophotometer. Infrared spectra were monitored with a Nicolet MX-S FT spectrophotometer. Magnetic susceptibility measurements in the polycrystalline state (room temperature) were performed on a Johnson Matthey magnetic susceptibility balance. Solution magnetic susceptibility was checked by the conventional NMR method[20] using Me_4Si. Elemental analyses were completed by Atlantic Microlab Inc., Atlanta, GA.

Table I. Summary of Crystal Data, Intensity Collection, and Structure Refinement Parameters for $(Ph_4P)_2[Ni_3(SCH(CH_3)COO)_4]$ (**2**)

formula (mol wt)	$C_{60}H_{56}O_8P_2S_4Ni_3$ (1270.70)
cryst color, form	greenish black blocks
a, Å	15.444 (5)
b, Å	21.507 (8)
c, Å	17.206 (6)
cryst system	orthorhombic
space group	*Pbca*
V, Å^3	5715 (3)
D_{calcd}, g cm^{-3}	1.48
D_{obsd}, g cm^{-3} [a]	1.47 (2)
Z	4
cryst dimens, mm	0.50 × 0.54 × 0.46
abs coeff, μ, cm^{-1}	11.16
radiation	Mo Kα (0.71069 Å) (graphite monochromator)
temp, °C	24
scan speed, deg/min	2.0–5.0 ($\theta/2\theta$ scan)
scan range, deg	1.0 below Kα_1 to 1.0 above Kα_2
bkgd/scan time ratio	0.5
no. of data collcd	3037
no. of unique data $F_o^2 > 3\sigma(F_o^2)$	1886
no. of variables	205
R,[b] %	4.57
R_w,[c] %	5.00
max Δ/σ in final least-squares cycle	0.001
largest resid electron dens, e/Å^3	0.40 (associated with C43)

[a] Determined by flotation in CCl_4/cyclohexane. [b] $R = \sum||F_o| - |F_c||/\sum|F_o|$. [c] $R_w = (\sum w(|F_o| - |F_c|)^2/\sum wF_o^2)^{1/2}$.

X-ray Data Collection and Reduction. Green-black blocks of **2** were obtained by slow diffusion of diethyl ether into a DMF solution. Diffraction experiments were performed on a four-circle Syntex $P2_1$ diffractometer with graphite-monochromatized Mo Kα radiation. The initial orientation matrix was obtained from 15 machine-centered reflections selected from a rotation photograph. These data were used to determine the crystal system. Partial rotation photographs around each axis were consistent with an orthorhombic crystal system. Ultimately, 62 high-angle reflections ($20° < 2\theta < 25°$) were used to obtain the final lattice parameters and the orientation matrix. Machine parameters, crystal data, and data collection parameters are summarized in Table I. The observed extinctions were consistent with the space group *Pbca*. $+h,+k,+l$ data were collected in one shell ($4.5° < 2\theta < 40°$). Three standard reflections were recorded every 197 reflections. Their intensities showed no statistically significant change over the duration of data collection. The data were processed by using the SHELX-76 program package.[21] A total of 1886 reflections with $F_o^2 > 3\sigma F_o^2$ were used in the refinement. No absorption correction was applied to the data.

Solution and Refinement of the Structure. Non-hydrogen atomic scattering factors were taken from literature tabulations.[22] The Ni atom positions were determined by use of the heavy-atom (Patterson) method. The remaining non-hydrogen atoms were located from successive difference Fourier maps. Refinement was carried out by using full-matrix least-squares techniques on F, minimizing the function $\sum w(|F_o| - |F_c|)^2$ where the weight w is defined as $4F_o^2/\sigma^2(F_o^2)$ and F_o and F_c are the observed and calculated structure factor amplitudes. In the final cycles of refinement, Ni, S, O, and P atoms were assigned anisotropic temperature factors. Carbon atoms were described with isotropic thermal parameters. Hydrogen atom positions were allowed to ride on the carbon to which they are bonded, assuming a C–H bond length of 0.95 Å. Hydrogen atom temperature factors were fixed at 1.10 times the isotropic temperature factor of the carbon atom to which they are bonded. In all cases, the hydrogen atom contributions were calculated but not refined. The following data are tabulated: positional parameters (Table II) and selected bond distances and angles (Table III). Thermal parameters (Table S1), hydrogen atom parameters (Table S2), bond distances and angles associated with the cation (Table S3), values of 10 $|F_o|$ and 10$|F_c|$

(10) Dance, I. G. *Polyhedron* **1986**, *5*, 1057.
(11) (a) Lane, R. W.; Ibers, J. A.; Frankel, R. B.; Papaefthymiou, G. C.; Holm, R. H. *J. Am. Chem. Soc.* **1977**, *99*, 84. (b) Watson, A. D.; Rao, C. P.; Dorfman, J. R.; Holm, R. H. *Inorg. Chem.* **1985**, *24*, 2820.
(12) (a) Tremel, W.; Krebs, B.; Henkel, G. *Inorg. Chim. Acta* **1983**, *80*, L31. (b) Tremel, W.; Krebs, B.; Henkel, G. *Angew. Chem., Int. Ed. Engl.* **1984**, *23*, 634. (c) Tremel, W.; Krebs, B.; Henkel, G. *J. Chem. Soc., Chem. Commun.* **1986**, 1527.
(13) Bonamico, M.; Dessy, G.; Fares, V.; Scaramuzza, L. *J. Chem. Soc., Dalton Trans.* **1975**, 2594.
(14) (a) Jicha, D. C.; Busch, D. H. *Inorg. Chem.* **1962**, *1*, 872. (b) Wei, C. H.; Dahl, L. F. *Inorg. Chem.* **1970**, *9*, 1878.
(15) Barrera, H.; Suades, J.; Perucaud, M. C.; Brainso, J. L. *Polyhedron* **1984**, *3*, 839.
(16) Gaete, W.; Ros, J.; Solans, X.; Font-Altaba, M.; Brianso, J. H. *Inorg. Chem.* **1984**, *23*, 39.
(17) Woodward, P.; Dahl, L. F.; Abel, E. W.; Crosse, B. C. *J. Am. Chem. Soc.* **1965**, *87*, 5251.
(18) Dance, I. G.; Scudder, M. L.; Secomb, R. *Inorg. Chem.* **1985**, *24*, 1201.
(19) Gill, N. S.; Taylor, F. B. *Inorg. Synth.* **1967**, *9*, 136.
(20) (a) Evans, D. F. *J. Chem. Soc.* **1959**, 2003. (b) Phillips, W. D.; Poe, M. *Methods Enzymol.* **1972**, *24*, 304.
(21) Sheldrick, G. M. "SHELX-76, Program for Crystal Structure Determination"; University of Cambridge: Cambridge, England, 1976.
(22) Cromer, D. T.; Waber, J. T. *International Tables for X-ray Crystallography*; Kynoch: Birmingham, England, 1974; Vol. IV.

Table II. Positional Parameters[a]

atom	x	y	z	atom	x	y	z
Ni1	0 (0)	0 (0)	0 (0)	Ni2	662 (1)	188 (0)	−1486 (1)
S1	128 (1)	−646 (1)	−1005 (1)	S2	−378 (1)	669 (1)	−929 (1)
P1	4136 (1)	−1164 (1)	560 (1)	O1	1597 (3)	−261 (3)	−1896 (3)
O2	2217 (4)	−1189 (3)	−2018 (4)	O3	1203 (4)	943 (2)	−1736 (3)
O4	1441 (4)	1919 (3)	−1327 (4)	C1	1169 (5)	−1074 (4)	−1016 (5)
C2	1040 (6)	−1774 (4)	−1016 (5)	C3	1705 (5)	−836 (4)	−1710 (5)
C4	160 (5)	1431 (3)	−870 (5)	C5	−445 (6)	1945 (4)	−1146 (6)
C6	1010 (5)	1433 (4)	−1343 (5)	C11	3389 (5)	−515 (3)	619 (4)
C12	3081 (5)	−330 (3)	1341 (4)	C13	2482 (5)	143 (4)	1387 (5)
C14	2185 (5)	428 (4)	725 (4)	C15	2505 (5)	260 (4)	11 (5)
C16	3123 (5)	−212 (3)	−48 (5)	C21	4503 (5)	−1243 (3)	−419 (4)
C22	3928 (5)	−1388 (3)	−1015 (4)	C23	4213 (6)	−1423 (4)	−1776 (5)
C24	5073 (6)	−1318 (4)	−1945 (5)	C25	5645 (6)	−1184 (4)	−1375 (5)
C26	5379 (5)	−1144 (4)	−611 (5)	C31	3607 (4)	−1868 (3)	879 (4)
C32	3394 (5)	−2342 (4)	368 (5)	C33	2958 (6)	−2860 (4)	657 (6)
C34	2777 (6)	−2907 (4)	1444 (5)	C35	3005 (5)	−2448 (4)	1944 (6)
C36	3429 (5)	−1926 (4)	1665 (5)	C41	5058 (5)	−1027 (4)	1171 (4)
C42	5641 (6)	−1523 (4)	1256 (5)	C43	6415 (7)	−1427 (5)	1650 (5)
C44	6600 (7)	−845 (4)	1946 (5)	C45	6023 (5)	−374 (4)	1872 (5)
C46	5243 (5)	−446 (4)	1468 (4)				

[a] Multiplied by 10^4.

Table III. Selected Bond Distances and Angles

	Distances (Å)		
Ni1–Ni2	2.783 (1)	Ni1–S1	2.228 (2)
Ni1–S2	2.228 (2)	Ni2–S1	2.141 (2)
Ni2–S2	2.137 (2)	Ni2–O1	1.875 (5)
Ni2–O3	1.875 (5)	S1–C1	1.852 (8)
S2–C4	1.840 (8)	O1–C3	1.287 (9)
O2–C3	1.218 (9)	O3–C6	1.288 (9)
O4–C6	1.240 (9)	C1–C2	1.52 (1)
C1–C3	1.54 (1)	C4–C5	1.52 (1)
C4–C6	1.54 (1)		
	Angles (deg)		
S1–Ni1–S2	82.5 (1)	S1–Ni2–S2	86.7 (1)
S1–Ni2–O1	90.5 (2)	S2–Ni2–O3	91.1 (2)
O1–Ni2–O3	91.0 (2)	Ni1–S1–Ni2	79.1 (1)
Ni1–S1–C1	113.2 (3)	Ni2–S1–C1	94.5 (2)
Ni1–S2–Ni2	79.2 (1)	Ni1–S2–C4	114.6 (3)
Ni2–S2–C4	96.7 (2)	Ni2–O1–C3	120.0 (5)
Ni2–O3–C6	119.0 (5)	S1–C1–C2	112.3 (6)
S1–C1–C3	108.0 (6)	C2–C1–C3	113.5 (7)
O1–C3–O2	125.0 (8)	O1–C3–C1	116.3 (7)
O2–C3–C1	118.7 (8)	S2–C4–C5	110.7 (6)
S2–C4–C6	110.9 (6)	C5–C4–C6	110.7 (7)
O3–C6–O4	125.2 (8)	O3–C6–C4	118.1 (7)
O4–C6–C4	116.6 (8)		

(Table S4), and perpendicular distances of the core atoms from the molecular planes (Table S5) have been deposited as supplementary material.

Results and Discussion

$(Ph_4P)_2[Ni_3(SCH(CH_3)COO)_4]$ (**2**) has been isolated from a reaction mixture containing $(Ph_4P)_2NiCl_4$ and 1.5 equiv of the thiolate (Ph_4P^+ salt) in acetonitrile. Formation of the trimeric complex appears to proceed via in situ generation of $[Ni(SCH(CH_3)COO)_2]^{2-}$ and subsequent coordination of two such units to Ni^{2+}. When $[NiCl_4]^{2-}$ is allowed to react with >2 equiv of thiolactate, a clear greenish brown solution with absorption maxima at 568 and 420 nm is obtained. So far, we have been unsuccessful in isolating any crystalline material from this solution. Addition of 0.33 equiv of $[NiCl_4]^{2-}$ to the greenish brown solution results in immediate precipitation of **2** in ~90% yield (eq 1).

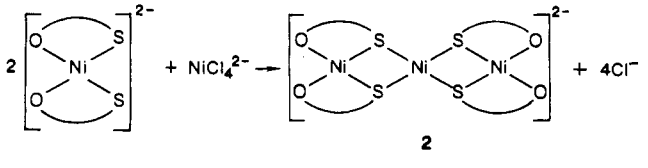

(1)

Trimeric nickel complexes of β-mercaptoethylamine (**3**)[14] and γ-mercaptopropylamine (**4**)[15] have been synthesized by analogous procedures.

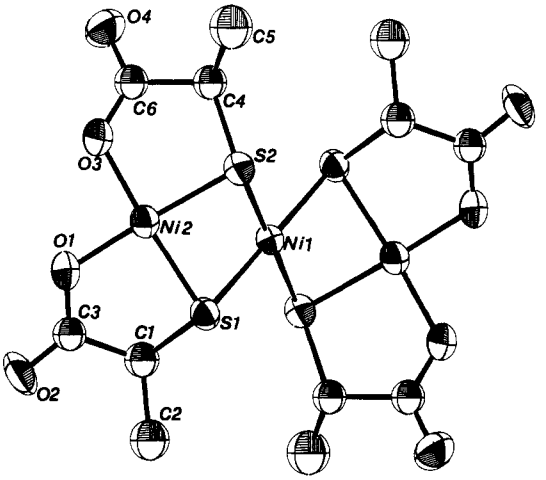

Figure 1. ORTEP drawing of the anion of **2** showing 30% thermal ellipsoids and the atom-labeling scheme. Hydrogen atoms are omitted for clarity.

Structure of $(Ph_4P)_2[Ni_3(SCH(CH_3)COO)_4]$ (2). The X-ray crystallographic study revealed that the crystals are made up of orthorhombic unit cells, each containing eight cations and four centrosymmetric anions. The closest approach between any pair of cation and anion is 2.585 Å (O2–H23). The geometry of the cation is typical,[23] and the angles and bond distances associated with it are supplied in Table S3 as supplementary material. An ORTEP drawing of the anion is shown in Figure 1, and selected bond distances and angles are collected in Table III. The coordination geometry around each nickel is pseudo square planar. The central nickel atom (Ni1), which sits on the center of symmetry of the anion, is coordinated to four sulfur atoms. Each of the two Ni2 atoms, positioned centrosymmetrically on either side of Ni1, is bonded to two oxygen and two sulfur atoms. The average Ni–S distance for Ni1 is 2.228 (2) Å, which is considerably longer than the average Ni2–S distance of 2.139 (2) Å. Such noticeable difference is typical of linear S-bridged nickel trimers.[11b,12b,14,15,24] In **2**, the difference (0.089 Å) is, however, higher than that observed in **4** (0.012 Å), **5** (0.026 Å), or **3** (0.056 Å). The average Ni–O bond length (1.875 (5) Å) is markedly

(23) Coucouvanis, D.; Swenson, D.; Baenziger, N. C.; Murphy, C.; Holah, D. G.; Sfarnas, N.; Simopoulos, A.; Kostikas, A. *J. Am. Chem. Soc.* **1981**, *103*, 3350.
(24) Stephan, D. W.; White, G. S., unpublished results.

Table IV. Absorption Spectral Data[a,b]

solvent	λ_{max}, nm (ϵ, M^{-1} cm^{-1})
acetonitrile	680 (1300), 555 (1350), 455 (3200), 315 sh[c] (13000)
DMF	670 (650), 565 (1200), 420 (3650), 330 sh (12000)
DMSO	570 (1200), 418 (4400), 335 sh (11500)
methanol	565 (1100), 420 (3600), 325 sh (12000)

[a] In solution, **2** is sensitive to oxygen. [b] Measurements were performed on freshly prepared solution. [c] Shoulder.

shorter than that noted for nickel(II) acetylacetonate[25] (average value 2.01 Å) and $[NiBr_2(S(CH_2CH_2OH)_2)_2]$ (2.046 (2) Å).[26] The bite angles of the 2-mercaptopropionate ligand at Ni2 are close to 90°. At Ni1, two S1–Ni–S2 angles are, however, quite smaller (82.5 (1)°). The Ni–Ni distance in **2** (2.783 (1) Å) is very similar to that observed for **3** (2.733 (7) Å).

In **2**, the NiS_4 and two NiS_2O_2 coordination planes form a "chair" conformation with the two symmetry-related NiS_2O_2 planes being parallel. The angle between the NiS_4 and NiS_2O_2 planes is 115°. This arrangement is quite similar to that found in **3**, where the corresponding angle is 109°. Coordination of S to the two adjacent nickel atoms through two different lone pairs, followed by steric adjustment, gives rise to this typical dihedral angle of ca. 110°.

It has been pointed out by Busch and co-workers[27] that the ready formation of **3** from $[NiL_2]$ species is suggestive of a cis structure for the monomeric complex. Trinuclear nickel(II) complexes could therefore be isolated only when the steric repulsion requirements of the ligand are relatively limited. Indeed, *N*,*N*-dimethyl-β-mercaptoethylamine forms only a monomeric nickel(II) complex in which the two bidentate ligands are in a trans configuration.[28] Clearly, limited steric requirements in the case of the 2-mercaptopropionate anion lead to the facile formation of **2** in the present work. Successful isolation of **2** also suggests that the monomeric complex anion $[Ni(SCH(CH_3)COO)_2]^{2-}$ (eq 1), not yet isolated, will adopt a cis configuration.

Properties. In the solid state, **2** is diamagnetic and relatively air-stable. When dissolved in deaerated acetonitrile, the trimeric complex exhibits band maxima (ϵ, M^{-1} cm^{-1}) at 680 (1300), 555 (1350), 455 (3200), and 315 nm (shoulder, 13000) (Figure 2, Table IV) and obeys Beer's law in the concentration range 0.01–0.3 mM. We assign the ~680-nm band to transition(s) associated with the NiS_4 chromophore.[29,30] The unusually high extinction coefficient might arise from pseudo-tetrahedral distortion of the NiS_4 chromophore in solution.[8a,30] Addition of up to 20 equiv of pyridine to a solution of **2** in acetonitrile does not bring about any change in the absorption spectrum. The trimeric structure appears to remain intact in such solution. However, when **2** is dissolved in DMF, the low-energy-band maximum shifts to 670 nm and the extinction coefficient drops to 650 (Figure 2). Addition of ~50% DMF to a solution of **2** in acetonitrile brings about a similar change in the electronic spectrum. The low-energy band is virtually absent in DMSO and methanol solution (Figure 2, Table IV). Variation in intensity of the ~680-nm band indicates that the trimeric complex decomposes readily in solvents like DMSO and MeOH. Similar behavior has been observed with **3** and **4**.[14,15] Clearly, the trimeric structure is stable in acetonitrile, and it is this solvent from which **2** has been isolated as microcrystalline solid. In the recrystallization step, diffusion of diethyl ether into DMF solution presumably causes preferential crystallization of the trimer.[31]

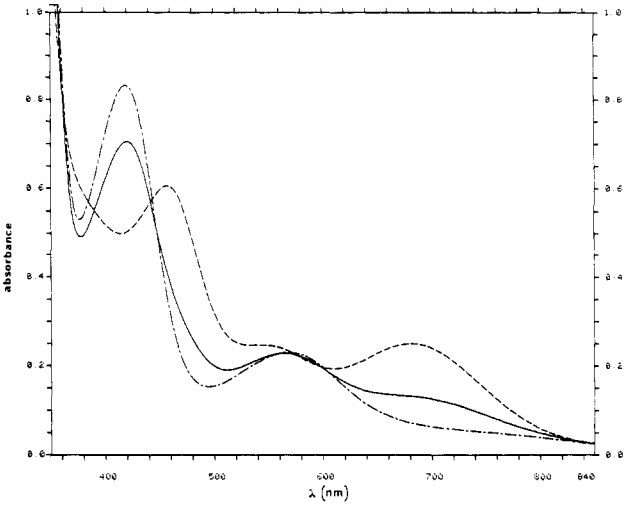

Figure 2. Absorption spectra of **2** (0.189 mM) in acetonitrile (---), DMF (—), and DMSO (-·-).

Preliminary results from magnetic susceptibility measurements on dilute solutions of **2** in CD_3CN indicate that the complex is diamagnetic in such solution. Marginal solubility of **2** in CD_3CN has restricted attempts to record high-quality NMR spectra and to obtain reliable solution susceptibility data.

Acknowledgment. This research was supported by a Faculty Research Committee Grant and the donors of the Petroleum Research Fund, administered by the American Chemical Society, at the University of California, Santa Cruz, CA. D.W.S. acknowledges financial support from the NSERC of Canada.

Registry No. **2**, 111004-82-1; $(Ph_4P)_2NiCl_4$, 111004-83-2.

Supplementary Material Available: Thermal parameters for non-hydrogen atoms (Table S1), hydrogen atom parameters (Table S2), bond distances and angles associated with the cation (Table S3), and perpendicular distances of the core atoms from the molecular planes (Table S5) (5 pages); values of $10|F_o|$ and $10|F_c|$ (Table S4) (7 pages). Ordering information is given on any current masthead page.

(25) Bullen, G. J.; Mason, R.; Pauling, P. *Inorg. Chem.* **1965**, *4*, 456.
(26) Udupa, M. R.; Krebs, B. *Inorg. Chim. Acta* **1981**, *52*, 215.
(27) Root, C. A.; Busch, D. H. *Inorg. Chem.* **1968**, *7*, 789.
(28) Girling, R. L.; Amma, E. L. *Inorg. Chem.* **1967**, *6*, 2009.
(29) Lever, A. B. P. In *Inorganic Electronic Spectroscopy*, 2nd ed.; Elsevier: Amsterdam, 1984; pp 535–537.
(30) Hendrickson, A. R.; Martin, R. L. *Inorg. Chem.* **1973**, *12*, 2582.
(31) The IR spectrum of the crude product from the reaction mixture (see Experimental Section) is identical with that of the recrystallized product. Analytical data for these two samples also confirm that the trimer can be recrystallized from DMF/ether.

Contribution from the Research School of Chemistry, The Australian National University, Canberra, ACT 2601, Australia

Electron-Transfer Reactions of Encapsulated Ruthenium, Manganese, Iron, and Nickel: Self-Exchange Rates for (3,6,10,13,16,19-Hexaazabicyclo[6.6.6]eicosane)metal(3+/2+) Couples

P. Bernhard*† and A. M. Sargeson*

Received February 20, 1987

The question of nonadiabaticity in electron-transfer (et) reactions of transition-metal complexes is continuing to attract attention,[1] and approaches to the "electronic factor" have been made experimentally[2] and theoretically.[3] The interest has been particularly stimulated by the fact that there exist some (large) discrepancies between observed and calculated et rate constants and that the classical, adiabatic theories of Marcus[4] and Hush[5] could not account for the large negative entropies of activation observed. Equally important has been the early realization that the ground-state electron self-exchange in most Co^{3+}–Co^{2+} systems is spin-forbidden.[6]

† Present address: California Institute of Technology, Pasadena, CA 91125.

